Nigerian Journal of Technology (NIJOTECH)
Vol. 37, No. 3, July 2018, pp. **758 – 769**

Print ISSN: 0331-8443, Electronic ISSN: 2467-8821
www.nijotech.com
http://dx.doi.org/10.4314/njt.v37i3.27

COIL- AND PHASE-FLUX-LINKAGE CHARACTERISTICS OF DUAL EXCITED PERMANENT MAGNET MACHINES EQUIPPED WITH DIFFERENT WINDING CONFIGURATIONS

C. C. Awah[1,*] and O. I. Okoro[2]
[1, 2,] DEPT. OF ELECTRICAL & ELECTRONICS ENGR., MICHAEL OKPARA UNIV. OF AGRIC., UMUDIKE, ABIA STATE, NIGERIA
E-mail addresses: [1]*ccawah@ieee.org,* [2]*profogbonnayaokoro@ieee.org*

ABSTRACT
The flux-linkage characteristics of dual excited permanent magnet (PM) machines equipped with concentrated windings of single- and double-layer types is investigated in this paper. This includes precise comparison of the coil and phase flux-linkage waveforms of the machines having different stator and rotor pole topologies. It is observed that, the developed machine having double layer-wound configuration have unipolar coil flux linkage waveforms, although with a resultant bipolar phase flux-linkage waveforms on summation, while their corresponding single layer-wound counterparts are characterised by both bipolar coil and phase flux-linkage waveforms. Also, the opposite coils of the machines having single-layer windings as well as even rotor pole topology produces coil flux-linkage waveforms whose shape and magnitude are identical and same; thus, resulting to more phase harmonics unlike their counterparts that are equipped with odd rotor poles and single-layer winding configuration whose coil waveforms are shifted, thereby resulting to effective cancellation of harmonics in the resultant phase waveforms. In general, the single-layer-wound machines exhibit higher peak-to-peak and fundamental flux-linkage values than their double-layer-wound equivalents.

Keywords: *Dual excitation, flux-linkage, single- and double-layer windings, rotor and stator pole combinations.*

1. INTRODUCTION
The shape and nature of flux-linkage and back-EMF waveforms of permanent magnet (PM) machines are important determinants in the design and analysis of electric machines, since they give insight on the output electromagnetic torque as well as the required control method (s) to be applied on the machines. A comparative study in [1] shows that the single-layer wound machines have better flux-weakening capability as well as higher fault-tolerant potential than their double-layer counterparts. However, the double-layer wound machines are good candidates for shorter end windings and hence improved efficiency, better or more sinusoidal electromotive force (EMF) waveforms, lower torque ripple and lower rotor losses due to their low magneto-motive force (MMF) components.

It is noted in [2], that surface-mounted permanent magnet machines (SPM) having single-layer wound topology exhibit larger inductance as well as more harmonic contents than their double-layer counterparts and this could be detrimental to the operational speed of the single-tooth wound machines. Hence, the double-layer wound machines have wider operating speed range. Thus, an enhanced flux-weakening potential is obtained in the double-layer-wound machines as mentioned in [3]. It is also proven in [3] that, the double-layer wound machines have lower core and eddy current losses relative to the single-layer-wound ones. Further reduction of losses would be obtained by adopting distributed kind of windings in place of the concentrated non-overlapping windings. It is shown in [4] that, the single-layer wound machines have higher winding factors and consequently are good candidates for larger torque-density compared to their double-layer equivalents. Li *et al* [5] show that the losses of fractional slot concentrated-winding PM machines reduces with increasing number of winding layers, although the lower winding-layer machines would produce higher electromagnetic output torque. In contrast, a study in [6] shows that the multi-layer wound machines are capable of producing larger torque than the single-layer ones, owing to their higher values of reluctance torque and saliency ratios. In addition, the multi-layer

***Corresponding author, tel: +234 – 803 – 422 – 1305**

wound machines have reduced torque ripple and enhanced overload withstand capability compared to the single-layer ones; albeit with increased mechanical complexity.

Furthermore, [7] demonstrates that the single-layer wound synchronous reluctance PM machines are characterized by significant amount of radial magnetic force on the rotor which could lead to heavy stress on the bearings, due to the resultant unbalanced magnetic pull. However, much reduction of these forces could be achieved by the use of additional flux-barriers on the rotor. It is also noted that, more sinusoidal as well as low amplitude of stator and rotor magnetic potentials are realized by adopting distributed windings in place of fractional-slot concentrated windings. Moreover, an improved analytical estimation of leakage flux and inductances of machines having single- and double-layer winding are proposed in [8] and [9], respectively. This approach is fast and consumes less time than the finite element (FEA) approach, although may not be entirely accurate since it is based on assumptions and approximations such as negligible magnetic saturation, etc. Moreover, it is demonstrated in [10] that, the torque and power density of axial flux PM machine is inversely related to the number of its winding-layers, i.e. the lower the number of layers the better its torque performance. However, a little compromise is made on the overall machine efficiency.

The schematic diagrams and flux-lines of the analyzed machines on open-circuit condition are shown in Figures 1 and 2, respectively.

2. METHODOLOGY AND MACHINE STRUCTURE

In this paper, the developed machines having different winding topologies as well as different rotor pole numbers are globally optimized by genetic algorithm using 2D finite element analysis (FEA) techniques for maximum average torque under fixed copper loss of 30W.

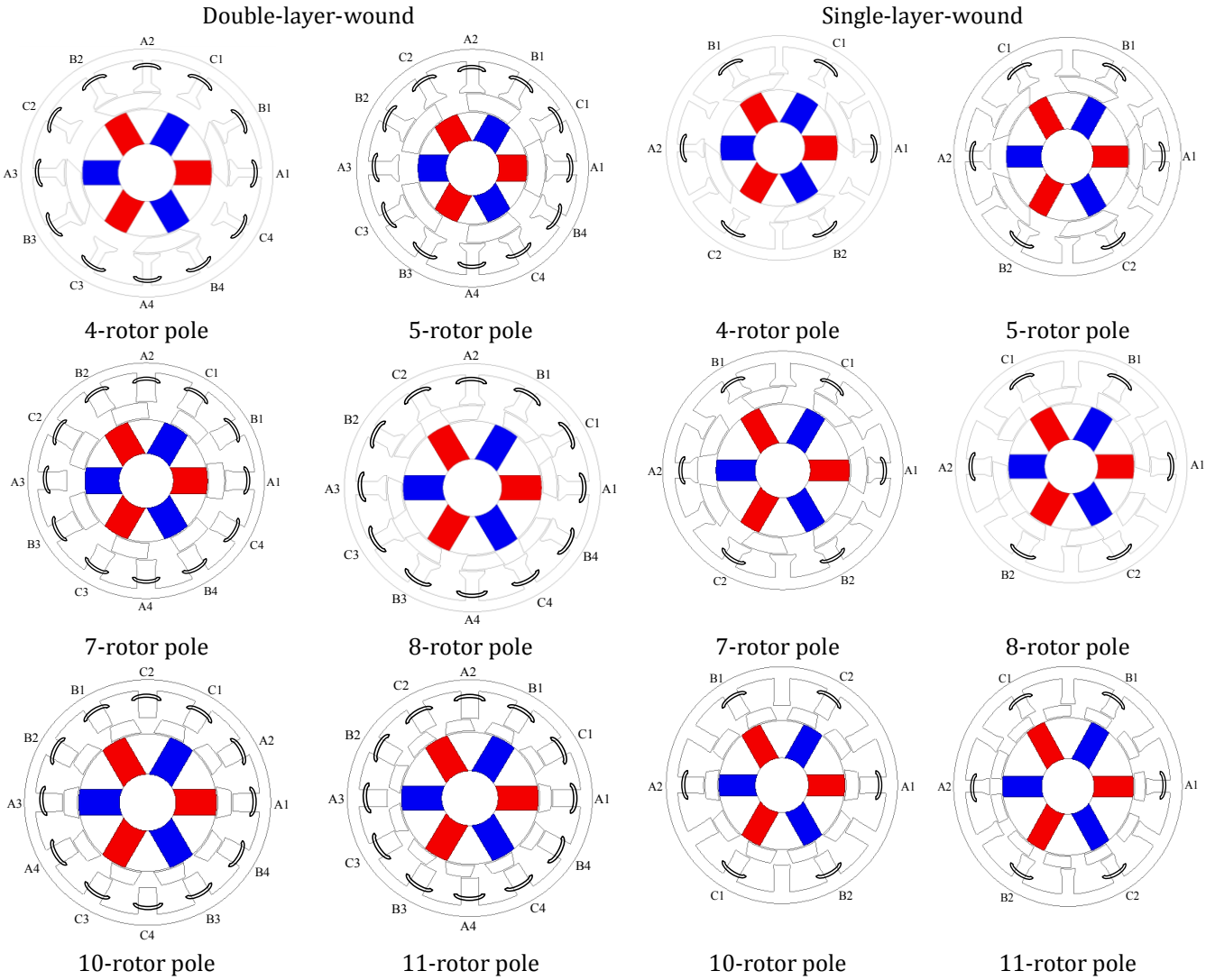

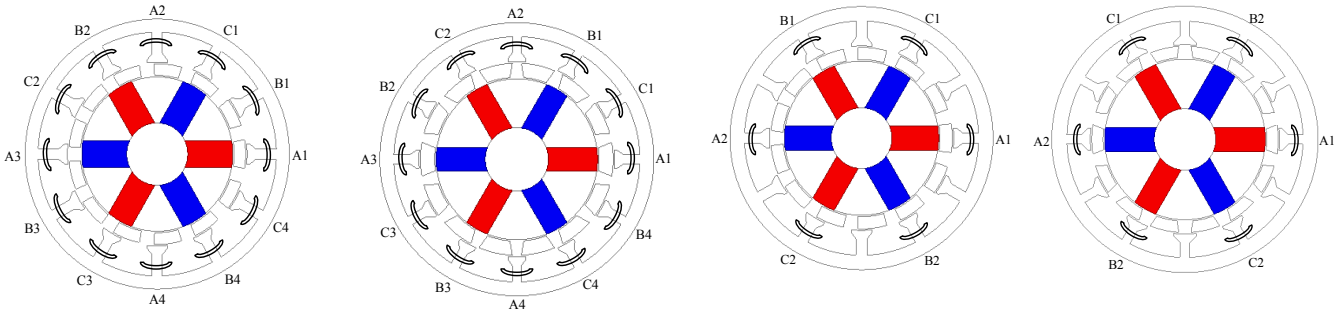

13-rotor pole 14-rotor pole 13-rotor pole 14-rotor pole

Figure 1: Schematic diagram of the developed machines with different winding configuration and pole numbers.

It is worth mentioning that, the series turns per phase of these machines are kept same in the analysis for fairness, the sum total being 72 turns per phase. The FEA design model is injected with three-phase sinusoidal current having 120deg. phase displacement, then operated at 400rpm speed on no-load condition in order to obtain the open-circuit flux-linkages and consequently, the other machine performances, such as induced electromotive force (EMF), torque etc. Nevertheless, we restricted this study mainly to the analysis of the flux-linkages analysis with few static torque results. Note also, that the used PM material in this work has a magnetic remanence of 1.2Tesla and relative permeability of 1.05.

The injected balanced three-phase sinusoidal currents are given by equations (1)-(3), however with I_{max}=0 for the considered open circuit condition in this paper.

$$I_A = I_{max} \times \sin(N_r\omega \times time + \emptyset_o) \quad (1)$$

$$I_B = I_{max} \times \sin(N_r\omega \times time - \frac{2 \times pi}{3} + \emptyset_o) \quad (2)$$

$$I_C = I_{max} \times \sin(N_r\omega \times time + \frac{2 \times pi}{3} + \emptyset_o) \quad (3)$$

where I_{max} = the maximum input current, N_r = the number of rotor poles, ω = the rotational speed, and $\emptyset_o$ =initial current advance angle.

3. RESULTS

The waveforms and spectra of the coil- and phase- flux-linkages of the analysed machines having different rotor-pole combinations with various rotor positions are shown in Figures 3-10. For the double-layer-wound machines, it is worth noting that the orthogonal coils always have different coil-flux linkage waveforms, while the diametrically opposite coils will have the same coil flux linkage if the number of rotor poles is even, otherwise, i.e. when the number of rotor poles is odd, their waveforms also differ. Similarly, for the single-layer-wound machines, there are only the diametrically opposite coils but no orthogonal coils in the same phase. In general, for the same rotor pole number, the double-layer-wound machines will have relatively lower amplitudes, compared to the single-layer-wound machines.

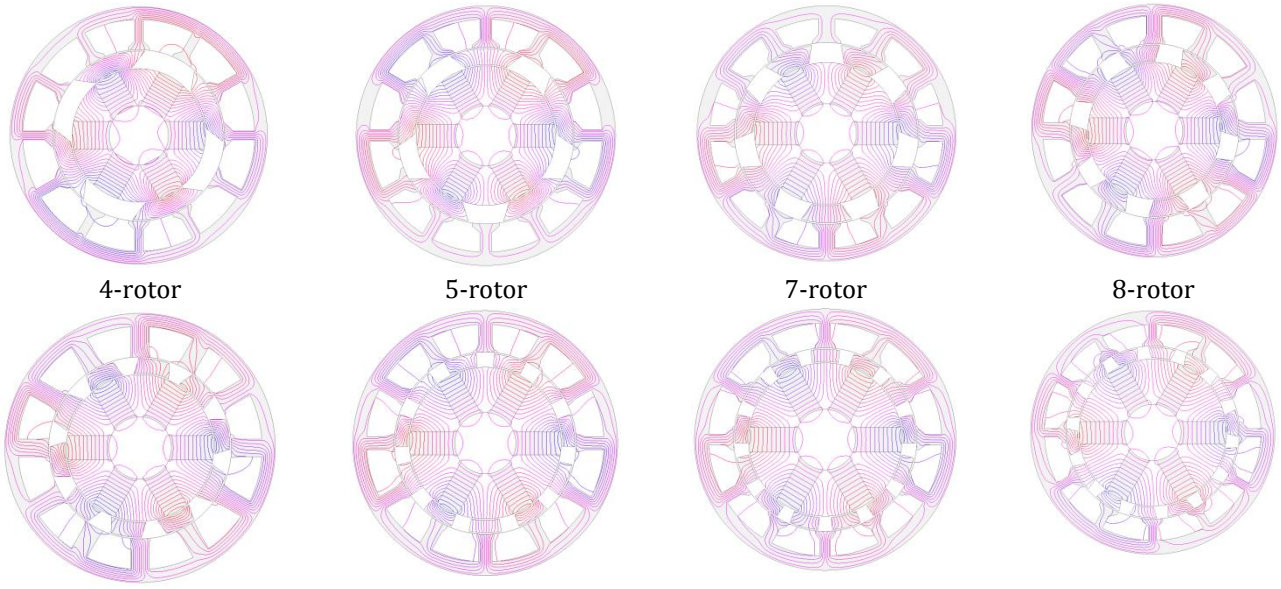

4-rotor 5-rotor 7-rotor 8-rotor

10-rotor 11-rotor 13-rotor 14-rotor

Figure 2: Open circuit flux distributions of the analysed machines.

The strength of the flux-lines in Figure 2 varies from tooth to tooth because, in each quarter of an electric cycle, since the resultant flux-linkages will depend upon the alignment of the rotor and stator teeth positions moving from positive maximum to zero, subsequently to negative maximum, afterwards back to zero, and finally to the initial amplitude. These positions correspond to positive direct-axis, positive quadrature-axis, negative direct-axis, and negative quadrature-axis, respectively as illustrated in [11]. In Figures 3-10, the first column is meant for the double-layer-wound topologies while the second column represents the single-layer-wound ones, in each case.

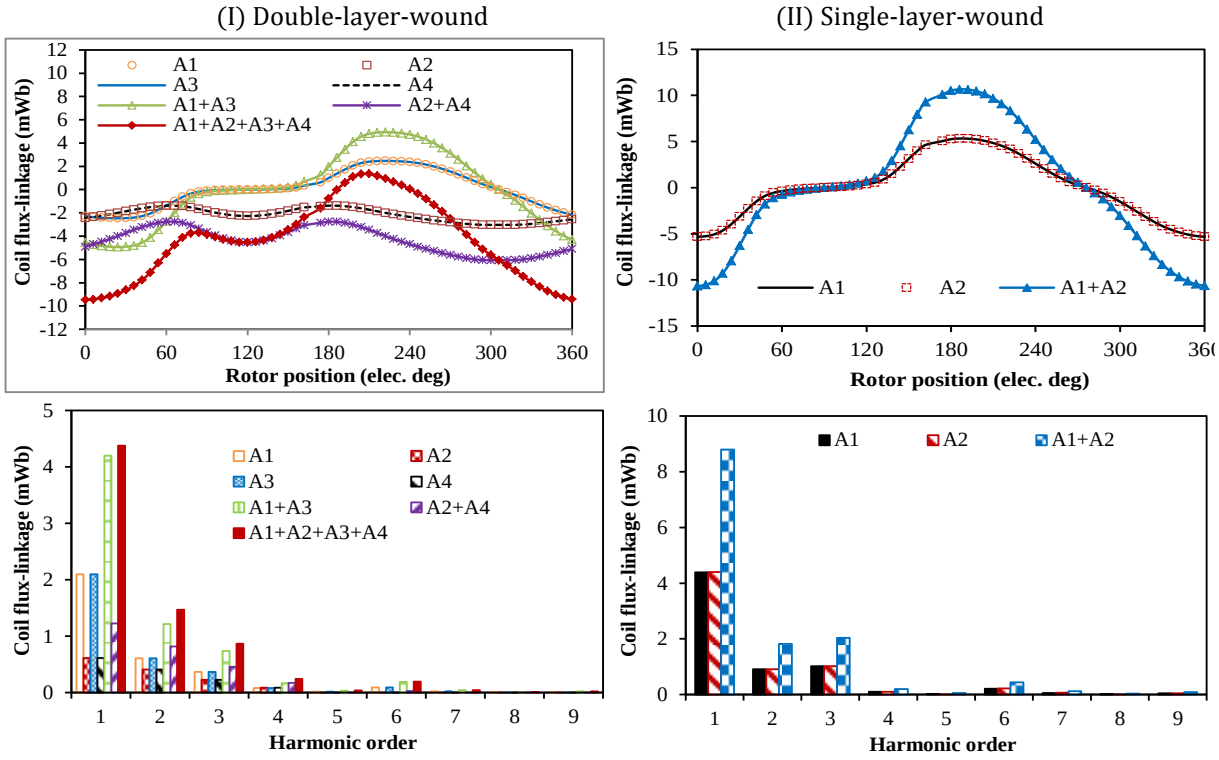

Figure 3: Comparison of open-circuit coil flux-linkages in analysed machines, 4-rotor pole.

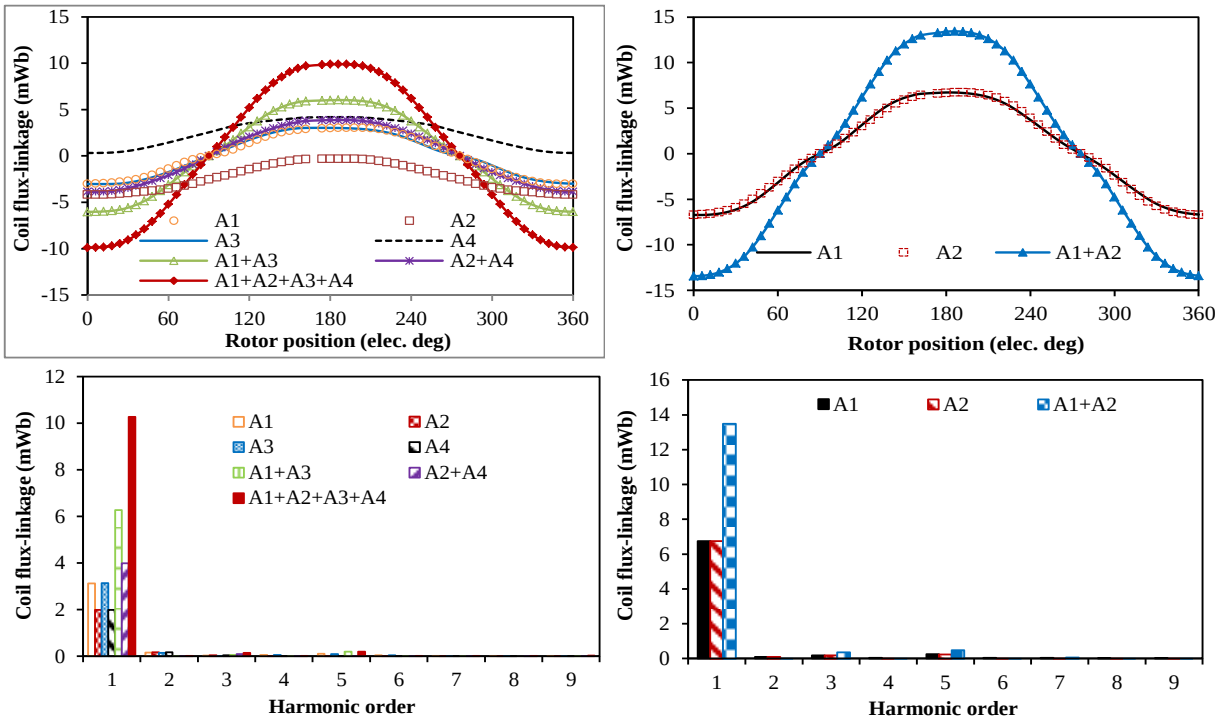

Figure 4: Comparison of open-circuit coil flux-linkages in analysed machines, 5-rotor pole.

It is worth noting that, the per phase coil group A1 and A3 of the double-layer-wound machines have larger amplitude in all the analysis than their complementary coil group, A2 and A4. This is because the flux-linkage waveforms of coils A2 and A4 are unipolar and in particular, they have different polarity in the odd-rotor pole machines, which in turn reduces the resultant flux-linkage significantly on summation. A typical example is seen in the 13-pole machine in which case, the sum of A2 and A4 flux-linkages is more or less negligible due to its unipolar waveforms with almost same amplitude and different polarity. Hence, the entire flux contribution in this case could be said to have been made by coils A1 and A3 only.

Moreover, the algebraic sum of coil flux-linkage which is equivalent to the phase flux-linkage, for example, in the even-rotor pole machines having all-pole-wound configuration are all unipolar. Note also, that the coil flux-linkage waveforms of coils belonging to the same phase of the machines having odd rotor pole number in addition to single-layer-wound configuration except that of 5-rotor pole will have similar coil flux-linkage waveforms with slight shift resulting to asymmetry owing to the varying scenario of their magnetic paths, as pointed out in [12]. It is worth noting that, the 2nd and 3rd harmonic components observed in the spectra of Figure 3, are most likely responsible for the unbalanced and distorted waveforms of the 4-rotor pole machine. However, in order to avoid asymmetric waveforms, proper selection of the rotor and stator poles is necessary and the condition for this selection which depends upon the highest common factor between the poles is clearly stated in [13].

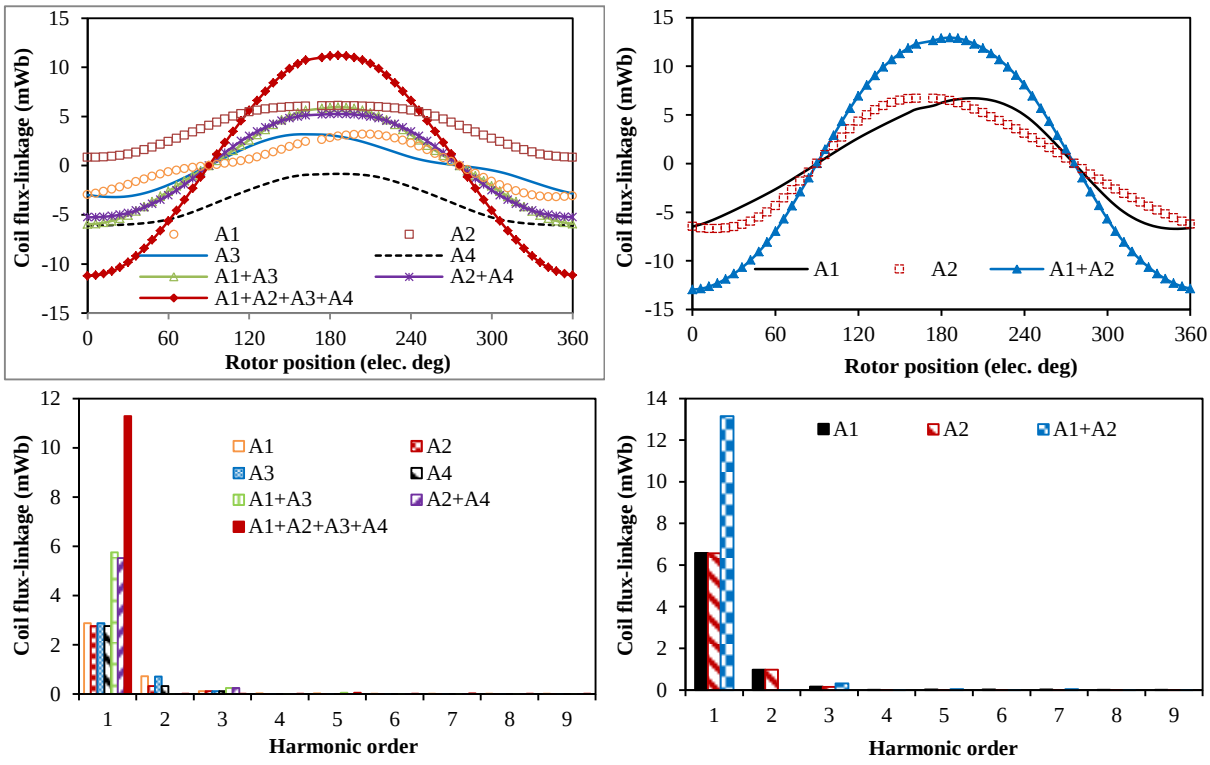

Figure 5: Comparison of open-circuit coil flux-linkages in analysed machines, 7-rotor pole.

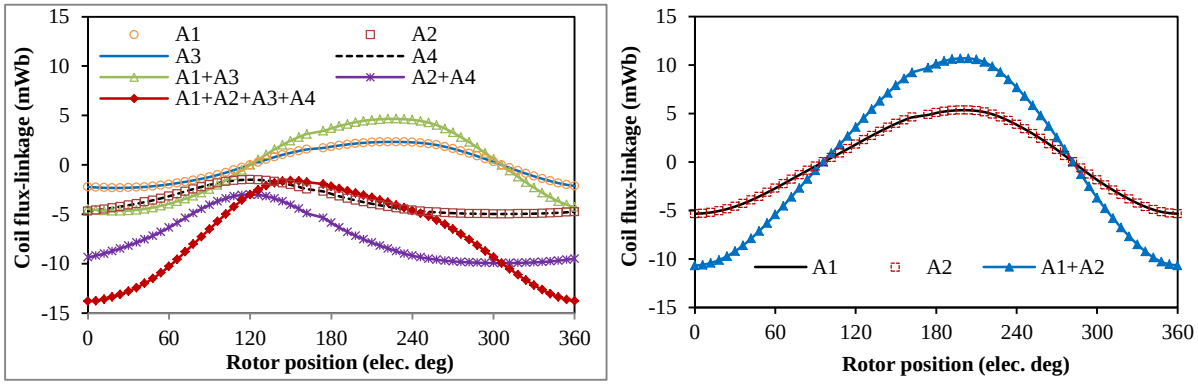

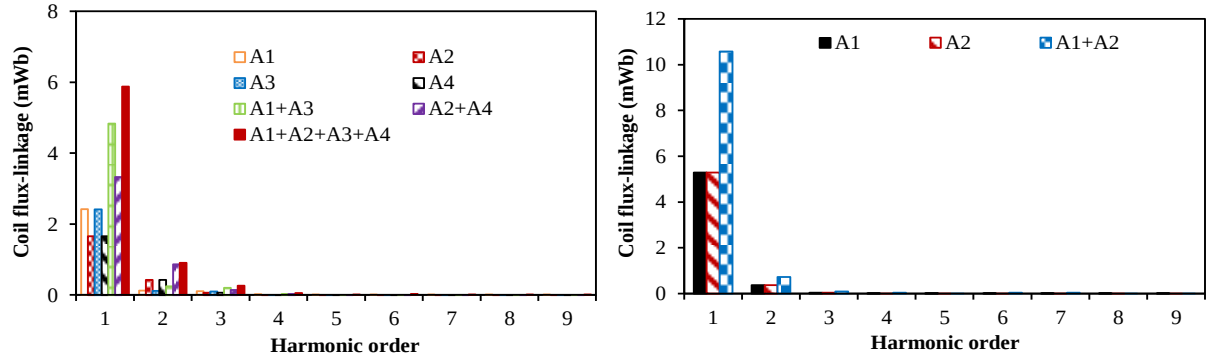

Figure 6: Comparison of open-circuit coil flux-linkages in analysed machines, 8-rotor pole.

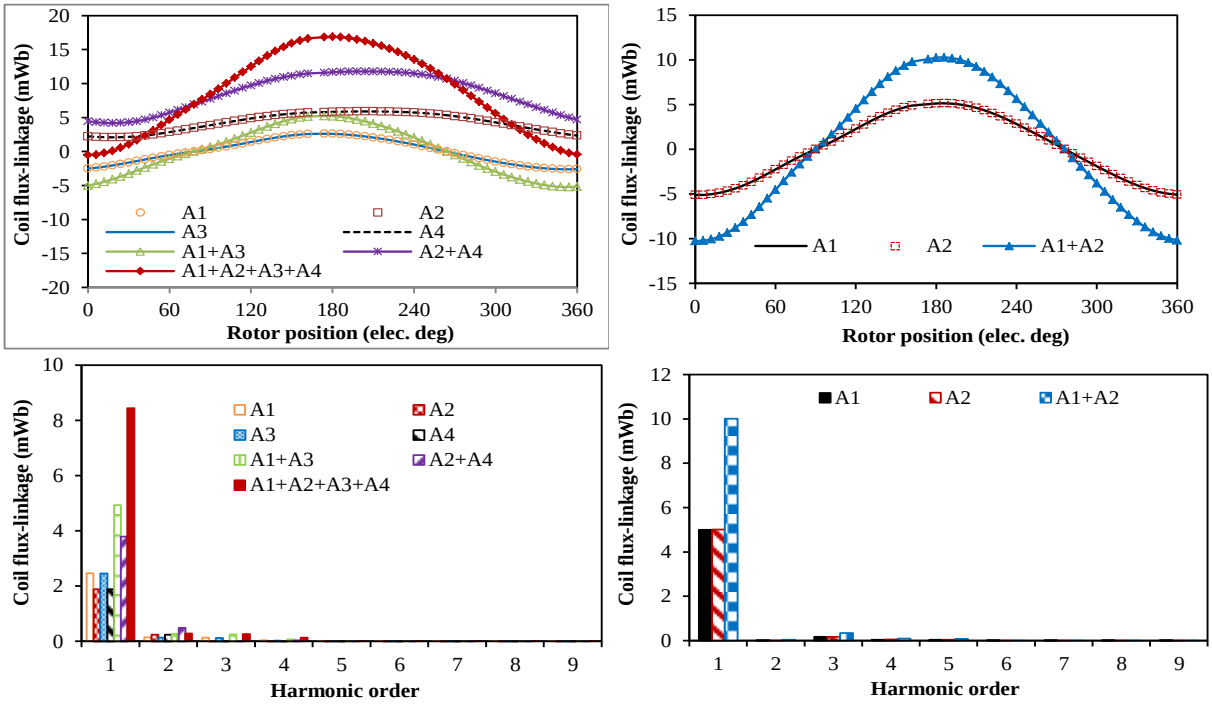

Figure 7: Comparison of open-circuit coil flux-linkages in analysed machines, 10-rotor pole.

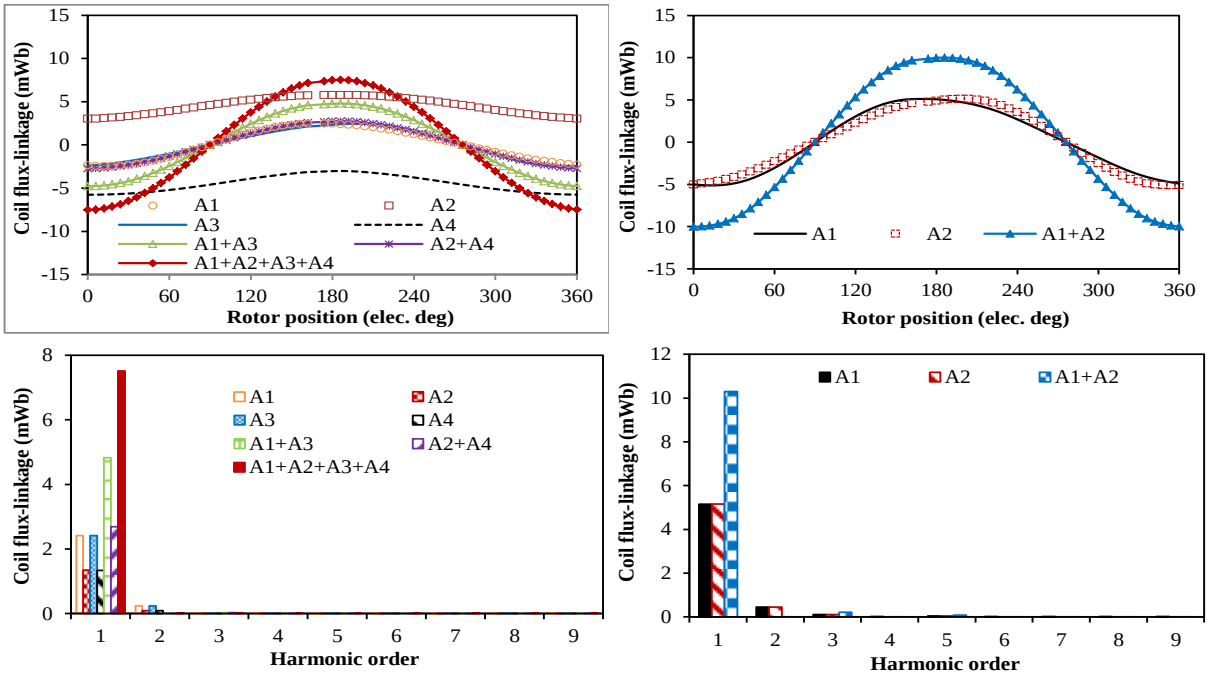

Figure 8: Comparison of open-circuit coil flux-linkages in analysed machines, 11-rotor pole.

Note also that, the coil flux-linkages of the even-rotor pole machines are identical, thus its individual coil harmonics are persistent in their respective phase spectra. In contrary, the coil waveforms of the odd-rotor pole machines are not identical thus they get rid-off the harmonics in their phase spectra by their cancellation effect on summation. More importantly, it should be noted that, although the waveforms of coils A2 and A4 are unipolar in the odd-rotor pole machines having double-layer-wound topology; their overall phase flux-linkage waveforms are bipolar. Also, it is worth noting that, the coil flux-linkage waveforms of A1 and A3 are bipolar in all the cases.

Although, not given in this paper for lack of space and scope, the odd rotor pole machines having single-layer windings usually have higher winding factor than their corresponding double-layer-wound counterparts. Thus, they have better performance than the double-layer ones; however they suffer from high torque ripple.

Figures 11 and 12 compare the phase flux-linkage waveforms and spectra of the anayzed double- and single-layer-wound machines having different rotor pole numbers. It can be clearly seen that, the phase flux-linkage waveforms of the even-rotor pole machines having double-layer-wound configuration are unipolar while their odd-rotor pole counterparts have bipolar waveforms. This means that the even-rotor pole machines having double-layer-wound topology would be better suited in DC applications, instead of AC direct-drive applications. Note also that, the 5- and 7-pole machines exhibit relatively more sinusoidal and symmetrical waveforms, as well as comparatively higher flux-linkage values than the other analysed machines owing to their high flux per pole characteristics.

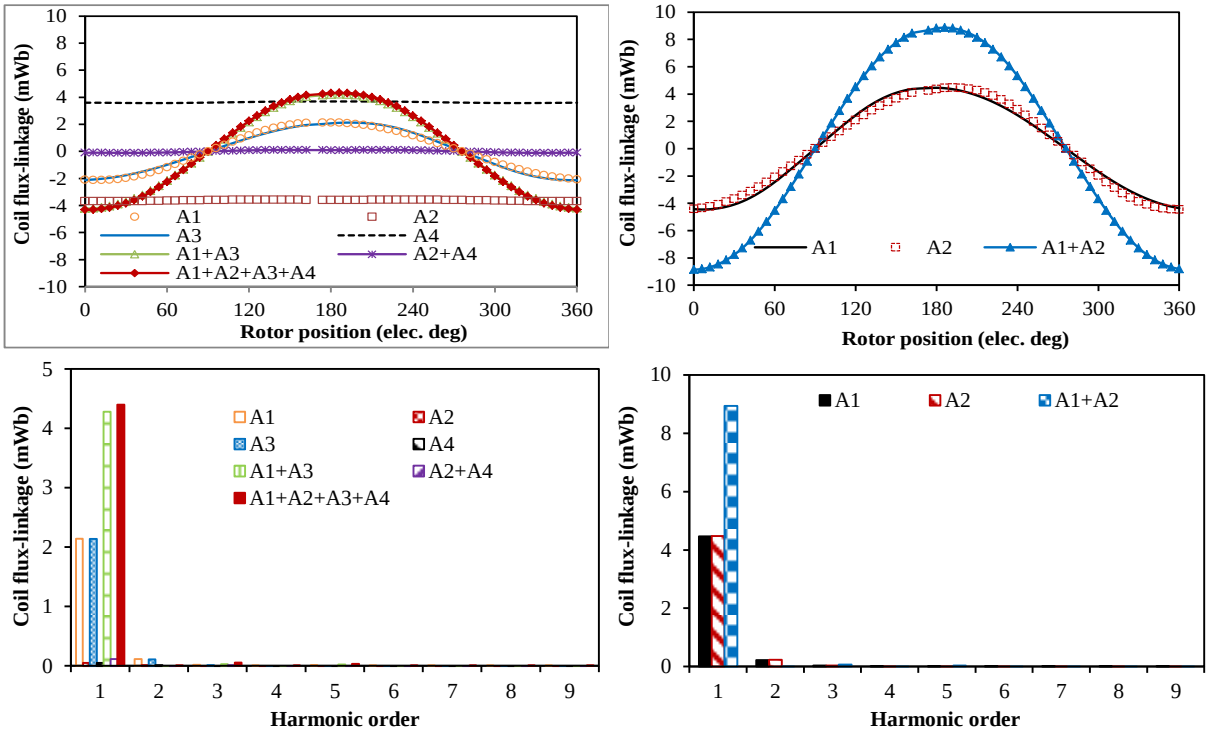

Figure 9: Comparison of open-circuit coil flux-linkages in analysed machines, 13-rotor pole.

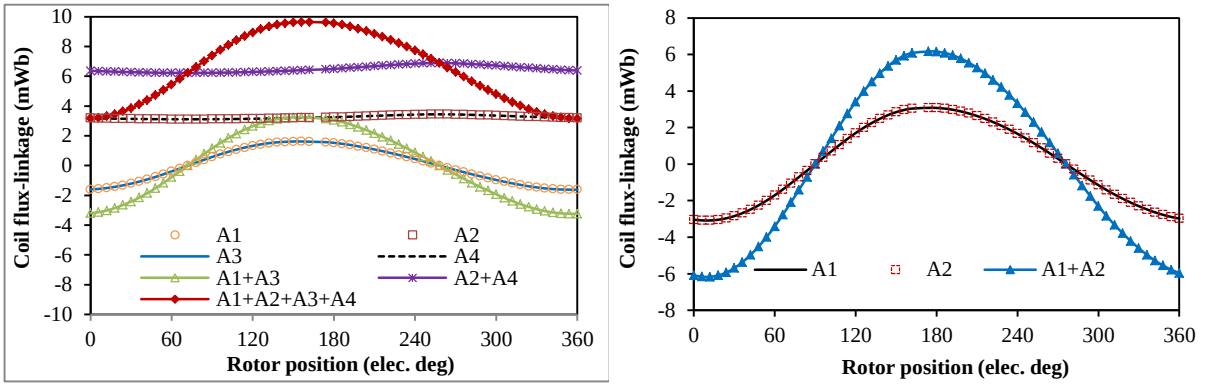

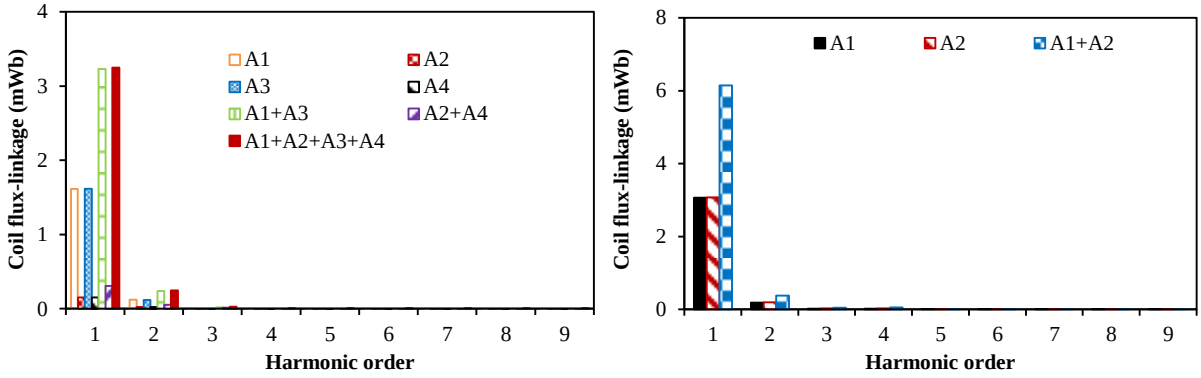

Figure 10: Comparison of open-circuit coil flux-linkages in analysed machines, 14-rotor pole.

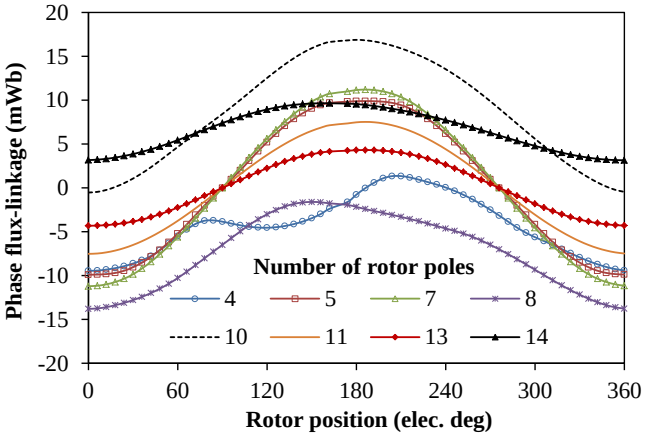

(a) Waveforms

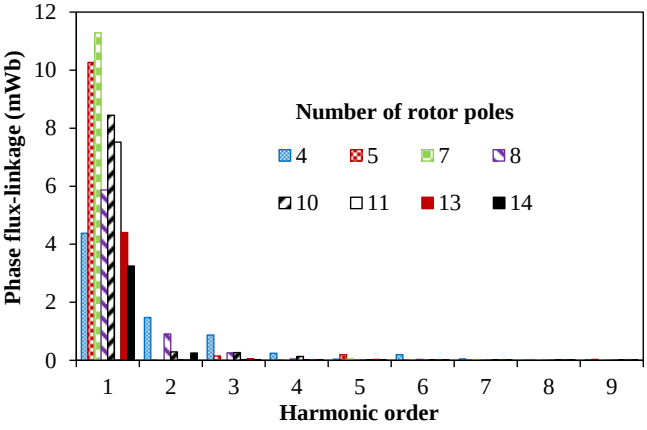

(b) Harmonics

Figure 11: Open-circuit flux-linkage variation with rotor position in double-layer wound machines.

Nevertheless, the single-layer-wound machines exhibit higher peak-to-peak and fundamental flux-linkage values than their double-layer-wound equivalents. It should also be noted that, the flux-linkage waveforms of the even rotor pole machines are both non-sinusoidal and asymmetric about the rotor position, in particular, the machine having four-rotor pole number whose waveforms are both unbalanced and well distorted. This implies that it would be unsuitable for brushless AC applications. In the spectra of Figures 11 and 12, it is obvious that 4-rotor pole machines contains undesirable 2nd and 3rd order harmonics in both types of winding topologies, which could lead to problems in the control and smooth operation of the machine, especially when delta type of winding connection is adopted. Moreover, the presence of 2nd order harmonics in the flux-linkage spectra of the 4- and 8-rotor pole machines implies that they would be characterized by higher torque ripple compared to the other anayzed machine configurations.

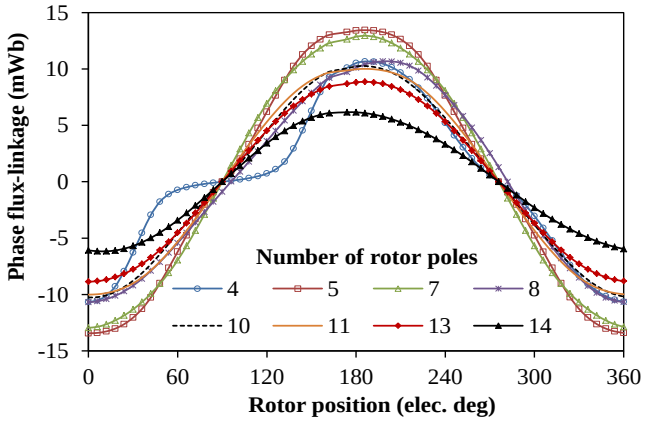

(a) Waveforms

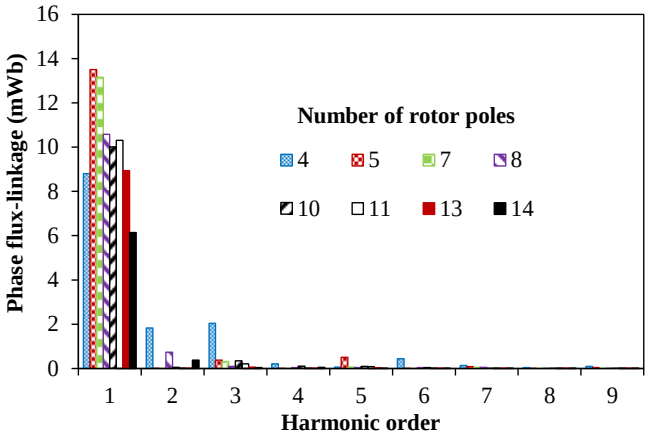

(b) Spectra

Figure 12: Open-circuit flux-linkage variation with rotor position in single-layer wound machines.

Similarly, the 3D FEA and 2D FEA comparison of the open-circuit phase flux–linkage and the static torque at 15A are shown in Figures 14 and 15, respectively. The analysis shows that there is about 14.32% and 18% discrepancies between the 3D and 2D FEA results of the no-load phase flux linkage and the static torque at 15A, respectively. This is because of the short active length of the analyzed machine i.e. 25mm, in addition to the end-winding issues. These problems will reduce in machines with larger stack or active length and larger outer machine diameter. It is worth noting that, the simulation results in Figures 14 and 15 are based upon the dimensions of the manufactured prototype. The 3D model of the dual-excited PM machine having 11-rotor-pole single layer-wound configuration is shown in Figure 13. The 11-rotor-pole machine is chosen since it has the best performance in terms of torque density amongst the investigated machines. Moreover, considering the enormous time that would be needed to perform 3D FEA analysis of the sixteen (16) different topologies compared in this paper.

Further, Figure 16 shows the cogging torque comparison of the eleven-rotor pole machine having alternate pole windings. It could be seen that the measured cogging is quite lower than the predicted one. This is in consonance with the result of the single-stator flux switching PM machine obtained in [14]. However, this could be as a result of irregularities in the prototyping especially as it relates to the uniformity of the air-gap circumference. Note also, that the measured cogging torque is not symmetric which is likely due to slight eccentricity of the rotor i.e. mechanical tolerance. More so, the initial rotor position of the measurement due to human error could also be a factor that may have influenced the results.

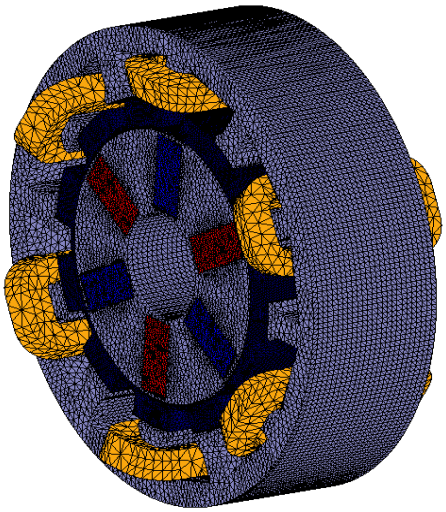

Figure 13: 3D mesh model of the analyzed machine, 11-rotor pole.

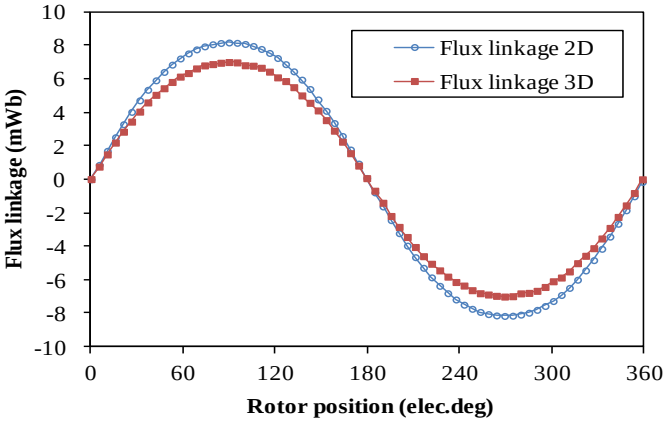

Figure 14: Comparison of phase flux-linkage, no load at 400rpm, 11-rotor-pole.

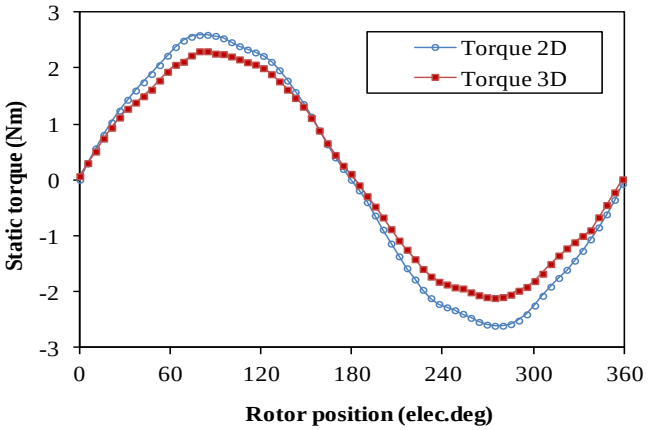

Figure 15: Comparison of static torque, 15 Amperes, 11-rotor pole.

It is worth noting that, the number of periods of cogging torque, CT_p in one electric rotation of the analyzed PM machine could be estimated using equation (4), as stated in [15].

$$CT_p = {N_s}/{GCD(N_s, N_r)} \quad (4)$$

where GCD is the greatest common divisor between the stator (N_s) and rotor pole (N_r) numbers.

The fabricated machine is shown in Figure 17.

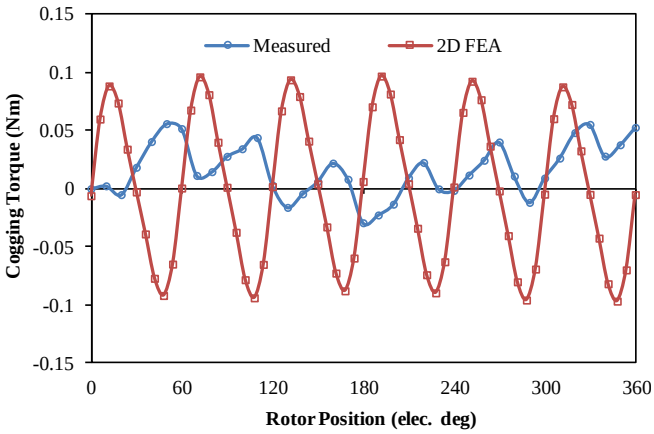

Figure 16: Comparison of cogging torque, 11-rotor-pole.

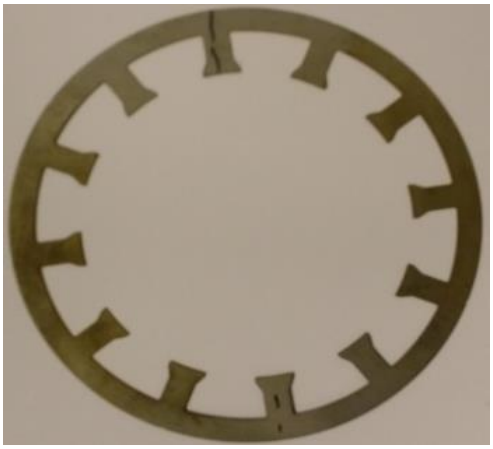

(a) Laminated stator steel

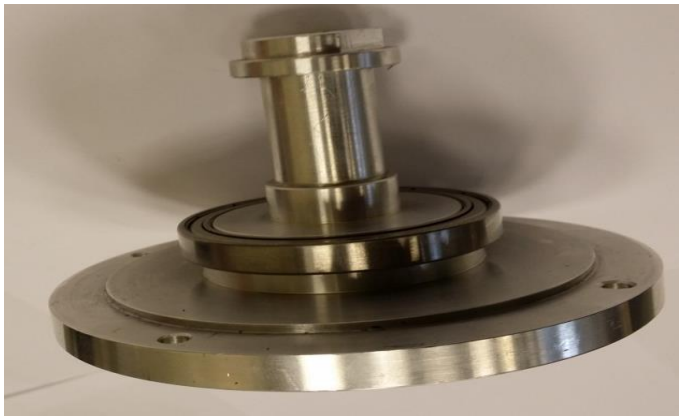

(b) Shaft with bearing

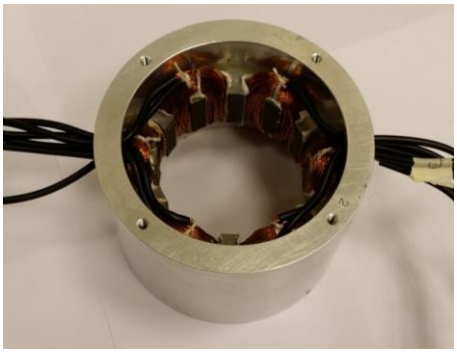

(c) Outer stator

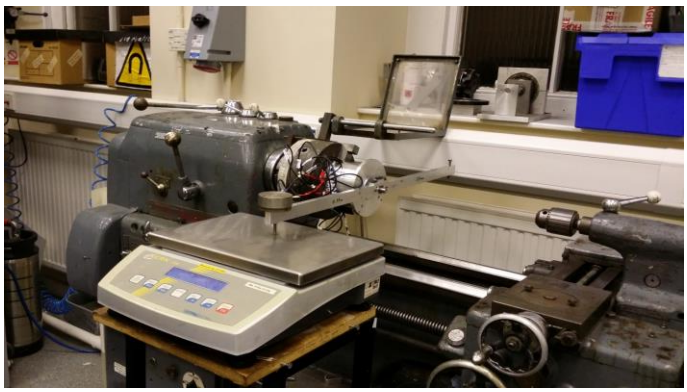

(d) Cogging torque test rig of the analyzed machine, 11-rotor alternate-pole-wound

Figure 17: Fabricated dual excited PM machine and the cogging torque experimental set-up.

The main machine parameters as well as the optimal geometric values of the investigated machines are listed in Tables 1 and 2.

Table 1: Parameters of the Analysed Double-Layer-Wound Machines

Item	Value							
Machine topology	All-pole-wound							
Rotor pole number, N_r	4	5	7	8	10	11	13	14
No. of outer stator slots, N_s	12							
No. of inner stator poles, P_s	6							
Number of phases, m	3							
No. of turns/coil	18							
Coils/phase	4							
Outer stator diameter (mm)	90							
Airgap length (mm)	0.5							
Active stack length (mm)	25							
Split ratio	0.65	0.63	0.67	0.67	0.69	0.67	0.67	0.71
Slot opening/slot pitch ratio	0.39	0.34	0.51	0.43	0.62	0.60	0.57	0.65
Rotor radial thickness (mm)	5.50	6.61	5.99	5.01	5.01	4.31	3.92	4.66
PM thickness (mm)	8.78	9.86	9.92	8.83	9.38	9.20	8.95	7.66
Outer rotor iron width/pitch ratio	0.56	0.64	0.53	0.66	0.47	0.52	0.66	0.79
Inner rotor iron width/pitch ratio	0.33	0.60	0.60	0.51	0.72	0.75	0.64	0.62
Stator back-iron thickness (mm)	4.19	4.55	3.66	3.96	3.93	4.24	4.39	4.60
Stator tooth width (mm)	3.20	4.89	6.83	4.78	6.77	6.64	3.49	3.00

Table 2: Parameters of the Analysed Single-Layer-Wound Machines

Item	Value							
Machine topology	Alternate-pole-wound							
Rotor pole number, N_r	4	5	7	8	10	11	13	14
No. of outer stator slots, N_s	12							
No. of inner stator poles P_s	6							
Number of phases, m	3							
No. of turns/coil	36							
Coils/phase	2							
Outer stator diameter (mm)	90							
Airgap length (mm)	0.5							
Active stack length (mm)	25							
Split ratio	0.66	0.68	0.71	0.68	0.67	0.68	0.70	0.71
Slot opening/slot pitch ratio	0.53	0.40	0.42	0.53	0.60	0.64	0.58	0.55
Rotor radial thickness (mm)	5.66	5.48	6.03	5.68	4.91	4.15	4.18	3.84
PM thickness (mm)	9.68	7.95	7.92	9.32	8.15	7.82	8.40	8.13
Outer rotor iron width/pitch ratio	0.59	0.67	0.64	0.64	0.54	0.64	0.66	0.71
Inner rotor iron width/pitch ratio	0.53	0.47	0.46	0.49	0.75	0.63	0.69	0.57
Stator back-iron thickness (mm)	4.46	4.61	4.49	4.11	4.37	4.64	4.93	5.10
Stator tooth width (mm)	3.12	4.11	5.64	5.86	5.91	4.55	3.69	3.01

4. CONCLUSION

Analysis of the coil and phase flux-linkage characteristics of PM machines having different winding topology as well as different stator/rotor pole combinations is presented. Overall, the machines having single-layer-wound topology have higher peak-to-peak and fundamental flux-linkage values than their double-layer-wound counterparts. More so, the analysed odd rotor pole machines have symmetric and more sinusoidal flux-linkage waveforms unlike their even rotor pole equivalents whose waveforms are asymmetric and non-sinusoidal about the rotor position. Furthermore, it is observed that the machines having double-layer windings in addition to even number of rotor poles exhibit unipolar phase flux linkage waveforms unlike their counterparts that are equipped with single-layer windings whose waveforms are bipolar.

5. ACKNOWLEDGEMENT

The first author would like to thank The Commonwealth Scholarship Commission, UK for the sponsorship to run a PhD programme at The University of Sheffield, UK, during which period this research was carried out.

6. REFERENCES

[1] A. M. EL-Refaie, "Fractional-slot concentrated-windings synchronous permanent magnet machines: opportunities and challenges," *IEEE Trans. Ind. Electron.*, vol. 57, no. 1, pp. 107-121, Jan. 2010.

[2] M. Popescu, D. G. Dorrell, D. Ionel and C. Cossar, "Single and double layer windings in fractional slot-per-pole PM machines – effects on motor performance," in proc. *IEEE Annual Conf. Ind. Electron.,* pp. 2055-2060, 2008.

[3] L. Chong, R. Dutta, M. F. Rahman, "A Comparative study of rotor losses in an IPM with single and double layer concentrated windings," in proc. *Int. Conf. Elect. Mach. Systs*. pp. 942-946, 2010.

[4] J. Yang, G. Liu, W. Zhao, Q. Chen, Y. Jiang, L. Sun, and X. Zhu, "Quantitative comparison for fractional-slot concentrated-winding configurations of permanent-magnet vernier machines," *IEEE Trans. Magn.*, vol. 49, no. 7, pp. 3826-3829, Jul. 2013.

[5] L. Qi, F. Tao, W. Xuhui, T. Xiang, and L. Ye, "A novel multi-layer winding design method for fractional-slot concentrated-windings permanent magnet machine, in proc. *IEEE Conf. Expo. Transp. Electrification,* pp. 1-5, 2014.

[6] Y. Wang, R. Qu, and J. Li, "Multilayer windings effect on interior PM machines for EV applications," *IEEE Trans. Ind. Appl.*, vol. 51, no. 3, pp. 2208-2215, May/Jun. 2015.

[7] H. Mahmoud and N. Bianchi, "Eccentricity in synchronous reluctance motors—part II: different rotor geometry and stator windings,"

IEEE Trans. Energy. Convers., vol. 30, no. 2, pp. 754-760, Jun. 2015.

[8] A. Tessarolo, "Leakage field analytical computation in semi-closed slots of unsaturated electric machines," *IEEE Trans. Energy Convers.*, vol. 30, no. 2, pp. 431-440, Jun. 2015.

[9] A. Tessarolo, "Analytical determination of slot leakage field and inductances of electric machines with double-layer windings and semiclosed slots," *IEEE Trans. Energy Convers.*, vol. 30, no. 4, pp. 1528-1536, Dec. 2015.

[10] A. Hemeida, and P. Sergeant, "Impact of single layer, double layer and four layer windings on the performance of AFPMSMs," in proc. *Int. Conf. Elect. Mach*. Systs. pp. 1-6, 2016.

[11] Z.Q. Zhu and J. T. Chen, "Advanced flux-switching permanent magnet brushless machines," *IEEE Trans. Magn.*, vol. 46, no. 6, pp.1447-1453, Jun. 2010.

[12] W. Hua, M. Cheng, Z.Q. Zhu, and D. Howe, "Analysis and optimization of back-EMF waveform of a novel flux-switching PM motor," *IEEE Trans. Energy Convers.*, vol. 23, no. 3, pp. 727-733, Sep. 2008.

[13] J.T. Chen, and Z. Q. Zhu, "Winding configurations and optimal stator and rotor pole combination of flux switching PM brushless AC machines," *IEEE Trans. Energy Convers.,* vol. 25, no. 2, pp. 293-302, Jun. 2010.

[14] J.T. Chen, Z.Q. Zhu, S. Iwasaki, and R. P. Deodhar, "Influence of slot opening on optimal stator and rotor pole combination and electromagnetic performance of switched-flux PM brushless AC machines," *IEEE Trans. Ind. Appl.*, vol. 47, no. 4, pp. 1681-1691, Jul./Aug. 2011.

[15] D. Wu, J. T. Shi, Z. Q. Zhu, and X. Liu, "Electromagnetic performance of novel synchronous machines with permanent magnets in stator yoke," *IEEE Trans. Magn.*, vol. 50, no. 9, pp. 8102009, Sept. 2014.